TECHNISCHE MECHANIK, 30, 4, (2010), 374 – 386
submitted: October 16, 2009

Homogenization methods for multi-phase elastic composites: Comparisons and benchmarks

B. Klusemann, B. Svendsen

Usually homogenization methods are investigated regarding the volume fraction of the inclusion. In this paper classical homogenization methods are recalled and compared on the basis of the contrast in the elastic properties of the constituents. This has a significant influence on the accuracy of the homogenization method. In addition two relatively new approaches, the ESCS and IDD method, are introduced and compared to more standard homogenization approaches. The analysis of these methods shows that the IDD method is an improvement due to its simple but universally applicable structure. A number of comparisons of these and other analytical approaches are carried out with the corresponding finite element results.

1 Introduction

The prediction of the macroscopic stress-strain response of composite materials is related to the description of their complex microstructural behavior exemplified by the interaction between the constituents. In this context, the microstructure of the material under consideration is basically taken into account by representative volume elements (RVE). In previous decades and especially in the absence of computers, analytical and semi-analytical approximations based on RVEs and mean-field homogenization schemes were developed. Mean-field homogenization methods were first developed in the framework of linear elasticity and are now well-established. These schemes provide efficient and straight forward algorithms for the prediction of, among other properties, the elastic constants (e.g. Mori-Tanaka method, Lielens method (Lielens, 1999), self consistent scheme). Moreover, the results obtained can be shown to be upper or lower bounds to the true solution of the underlying problem in most cases (e.g. Voigt-Reuss, Hashin-Shtrikman bounds). (see e.g., Gross and Seelig, 2001; Nemat-Nasser and Hori, 1999; Pierard et al., 2004).

All these methods are based on two steps to predict the macroscopic response. In a first step, a local problem for a single inclusion is solved in order to obtain approximations for the local field behavior as outlined by Eshelby for elastic fields of an ellipsoidal inclusion (Eshelby, 1957). The second step consists of averaging the local fields to obtain the global ones (e.g. Mercier and Molinari, 2009).

In this context, the main requirements on homogenization methods for predicting the effective properties, according to Zheng and Du (2001) are

a) a simple structure which can be solved explicitly, such that a physical interpretations for the behavior of all the components involved is possible;

b) a valid structure for multiphase composites with various inclusion geometries, isotropy and anisotropies;

c) an accurate model for the influence of various inclusion distributions and interactions between inclusions and their immediately surrounding matrix.

However, none of the aforementioned methods is really able to fulfill these requirements completely. The major disadvantages of these methods are exemplified by the fact that inclusion distributions are unaccounted for and that the properties of the surrounding matrix material does not enter these methods directly.
An interesting approach was presented by Guinovart-Díaz et al. (2005), namely the recursive asymptotic homogenization scheme (RAHS), which takes the variation of properties around cylindrical fibers into account by using multi-phase fibrous elastic composites, wherein the constituents exhibit transverse isotropy.

A new micromechanical model has been proposed by Zheng and Du (2001), namely the so-called effective self-consistent scheme (ESCS), which is based on the three-phase model which corresponds to the generalized self-consistent method (GSCS) (see Christensen, 1990). In the three-phase model, the inclusion is embedded in a matrix which itself is embedded in an unbound, initially unknown effective medium. This GSCS method fulfills requests b) and c) but is still rather complicated in terms of its application due to its implicit structure and it is also restricted to spherical or cylindrical inclusion. The ESCS overcomes the restriction to spherical and cylindrical inclusions. It still fulfills the requests b) and c) but has also a complicated structure. A simplified and explicit version of the ESCS method, which is referred to as the Interaction Direct Derivative (IDD) estimate was proposed satisfying all three requests. This method has a very simple structure with clear physical meaning of the single constituent parts. (Zheng and Du, 2001; Du and Zheng, 2002) show results for void distribution, although the formulation is also valid for spherical inclusions. This encourages a first discussion of this method regarding the inclusion as well as its comparison to classical homogenization schemes presented in this paper.

In many papers dealing with classical homogenization methods results in terms of effective material properties are presented depending upon the volume fraction of the inclusion. Here, we additionally present the results and compare different homogenization methods in terms of the ratio of stiffness of the different constituents, respectively.

The outline of the paper is as follows: In Section 2, basic mean-field homogenization methods are briefly discussed. Section 3 provides an overview on the ESCS and IDD approach. A comparison of different homogenization schemes with FE-results for different volume fraction of the inclusion as well as different stiffness ratios are provided in Section 4. The paper concludes in section 5 with a summary and outlook.

2 Review of some standard homogenization methods

In this section we consider linear elastic composites under isothermal conditions. Primarily, consider a macroscopic material point at a position $\boldsymbol{X}$ in a fixed Cartesian frame. In linear elasticity the macroscopic stresses $\boldsymbol{T}^{\mathrm{macro}}$ and strains $\boldsymbol{E}^{\mathrm{macro}}$ are related via the macroscopic elasticity tensor $\mathcal{C}_{\mathrm{macro}}$ with

$$\boldsymbol{T}^{\mathrm{macro}} = \mathcal{C}_{\mathrm{macro}} \boldsymbol{E}^{\mathrm{macro}}. \tag{1}$$

Homogenization procedures are mainly based on the definition of a local surrounding of a macroscopic material point with volume V and the boundary ∂V. This volume V represents a characteristic part of the material which is sufficient to describe its structure and behavior, respectively. This implies that the size of heterogeneities at the microlevel has to be one scale smaller than the size of the volume V of the macropoint. As it was shown by Nemat-Nasser and Hori (1999) and Gross and Seelig (2001) the Hill-Mandel condition is fulfilled by applying linear displacements, periodic boundary conditions or uniform tractions on ∂V. Therefore the average strain in the volume V is equal to the macro strain.

The previous explanation emphasizes that the macro elasticity tensor $\mathcal{C}_{\mathrm{macro}}$ averages out the heterogeneities on the microlevel and characterizes a homogeneous behavior at the macroscopic level. Hence, it is also referred to as effective elasticity tensor $\mathcal{C}^*$, and the stress-strain relation at the macroscale can be rewritten to

$$\langle \boldsymbol{T} \rangle = \mathcal{C}^* \langle \boldsymbol{E} \rangle, \tag{2}$$

for a multiphase composite consisting of n phases, $c_\alpha = V_\alpha / V$ denotes the volume fraction of each phase α with respect to the total volume V of the RVE, which are subjected to the restriction $\sum_{\alpha=1}^{n} c_\alpha = 1$.

We restrict the composite to the matrix-inclusion type with perfect interfacial bonds between inclusions and their immediate surrounding matrix. The matrix phase is labeled by M and the inclusion is assumed to be of type-i and therefore labeled by i. The volume V at the microlevel is subjected to linear boundary displacements which corresponds to a macroscopic strain $\boldsymbol{E}^0$. The microscopic strain within the RVE depends upon an initially unknown fourth-order tensor $\mathcal{A}(\boldsymbol{x})$ with

$$\boldsymbol{E}(\boldsymbol{x}) = \mathcal{A}(\boldsymbol{x}) \boldsymbol{E}^0 \tag{3}$$

referred to as concentration tensor. In the following, $\mathcal{A}$ describes the volume average of $\mathcal{A}(x)$. As this average is done phase-wise, this results in phase wise constant concentration tensors $\mathcal{A}_\alpha$. Hence, the effective elasticity tensor can be calculated via

$$\mathcal{C}^* = \sum_{\alpha=1}^{\mathrm{n}} c_\alpha \mathcal{C}_\alpha \mathcal{A}_\alpha. \tag{4}$$

For the special case of an ellipsoidal inclusion in an infinite matrix, the Eshelby solution can be used to determine the so far unknown concentration tensors $\mathcal{A}_\alpha$. As shown by many authors (e.q Gross and Seelig, 2001; Nemat-Nasser and Hori, 1999), the strain in the inclusion can be calculated by

$$\boldsymbol{E}^{\mathrm{I}} = \mathcal{A}_{\mathrm{I}}^0 \boldsymbol{E}^0 = \left[\mathcal{I} + \mathcal{S}\mathcal{C}_{\mathrm{M}}^{-1}(\mathcal{C}_{\mathrm{I}} - \mathcal{C}_{\mathrm{M}})\right]^{-1} \boldsymbol{E}^0 = const \tag{5}$$

where $\mathcal{I}$ designates the fourth-order symmetric identity tensor, $\mathcal{C}_{\mathrm{M}}$ the elasticity tensor of the matrix, $\mathcal{C}_{\mathrm{I}}$ the elasticity tensor of the inclusion and $\mathcal{S}$ the Eshelby tensor. In general, the Eshelby tensor $\mathcal{S}$ has both minor symmetries but no major symmetry. Results for ellipsoidal inclusion can be found in Mura (1982). For the special case of a spherical inclusion and isotropic material the Eshelby tensor $\mathcal{S}$ can be calculated via

$$\mathcal{S} = \frac{1}{3}\alpha \boldsymbol{I} \otimes \boldsymbol{I} + \beta(\boldsymbol{I} \square \boldsymbol{I} - \frac{1}{3}\boldsymbol{I} \otimes \boldsymbol{I}) \tag{6}$$

with

$$\alpha = \frac{1+\nu}{3(1-\nu)} \qquad \beta = \frac{2(4-5\nu)}{15(1-\nu)} \tag{7}$$

where ν is the Poisson's ratio of the matrix material. Here, $\boldsymbol{I}$ represents the second order identity tensor and we make use of the tensor products $(\boldsymbol{A} \otimes \boldsymbol{B})\boldsymbol{C} := (\boldsymbol{B} \cdot \boldsymbol{C})\boldsymbol{A}$ and $(\boldsymbol{A} \square \boldsymbol{B})\boldsymbol{C} := \boldsymbol{A}\boldsymbol{C}\boldsymbol{B}$ of any second-order tensors $\boldsymbol{A}, \boldsymbol{B}, \boldsymbol{C}$.

The same results as for strain boundary conditions can be obtained by applying uniform stress boundary conditions at the boundary of the volume V which correspond to a macroscopic stress $\boldsymbol{T}^0$. The microscopic stress in the volume V is related by a unknown fourth-order tensor $\mathcal{B}$ with

$$\boldsymbol{T}(x) = \mathcal{B}(x)\boldsymbol{T}^0 \tag{8}$$

being the concentration tensor. In the following $\mathcal{B}$ describes the volume average of $\mathcal{B}(x)$, where this results in phase wise constant concentration tensors $\mathcal{B}_\alpha$. Therefore the effective elasticity tensor can be calculated via

$$\mathcal{C}^* = \left(\sum_{\alpha=1}^{\mathrm{n}} c_\alpha \mathcal{C}_\alpha \mathcal{A}_\alpha \right)^{-1}. \tag{9}$$

In the following subsections some well-known homogenization schemes as well as two relatively new methods are depicted. Schematic illustrations concerning these schemes are given in Figure 1.

2.1 Mori-Tanaka method

The Mori-Tanaka method approximates the interaction between the phases by assuming that each inclusion i is embedded, in turn, in a infinite matrix that is remotely loaded by the average matrix strain $\boldsymbol{E}_{\mathrm{M}}$ or average matrix stress $\boldsymbol{T}_{\mathrm{M}}$, respectively. Therefore the strain in the single inclusion can be calculated by

$$\boldsymbol{E}_i^{\mathrm{I}} = \mathcal{A}_{\mathrm{I},i}^0 \boldsymbol{E}^{\mathrm{M}}, \tag{10}$$

where the influence tensor $\mathcal{A}_{\mathrm{I},i}^0$ is given by

$$\mathcal{A}_{\mathrm{I},i}^0 = \left[\mathcal{I} + \mathcal{S}_{\mathrm{M}}\mathcal{C}_{\mathrm{M}}^{-1}(\mathcal{C}_{\mathrm{I},i} - \mathcal{C}_{\mathrm{M}})\right]^{-1}. \tag{11}$$

In the case of ellipsoidal inclusions, the Mori-Tanaka homogenization approach leads to $\boldsymbol{E}_{\mathrm{I},i} = \mathcal{A}_{\mathrm{I(MT)},i}^0 \boldsymbol{E}^0$, where $\mathcal{A}_{\mathrm{I(MT)},i}$ is obtained by

$$\mathcal{A}_{\mathrm{I(MT)},i} = \left[c_i \mathcal{I} + c_{\mathrm{M}} (\mathcal{A}_{\mathrm{I},i}^0)^{-1} + \sum_j c_j \mathcal{A}_{\mathrm{I},j}^0 (\mathcal{A}_{\mathrm{I},i}^0)^{-1} \right]^{-1}. \tag{12}$$

With this results we can calculate the effective elasticity tensor

$$\mathcal{C}_{(\mathrm{MT})}^* = \mathcal{C}_{\mathrm{M}} + \sum_i c_i (\mathcal{C}_{\mathrm{I},i} - \mathcal{C}_{\mathrm{M}}) \mathcal{A}_{\mathrm{I(MT)},i}. \tag{13}$$

In Benveniste (1987) the method is interpreted in the sense that "each inclusion behaves like an isolated inclusion in the matrix seeing $\boldsymbol{E}_{\mathrm{M}}$ as a far-field strain".

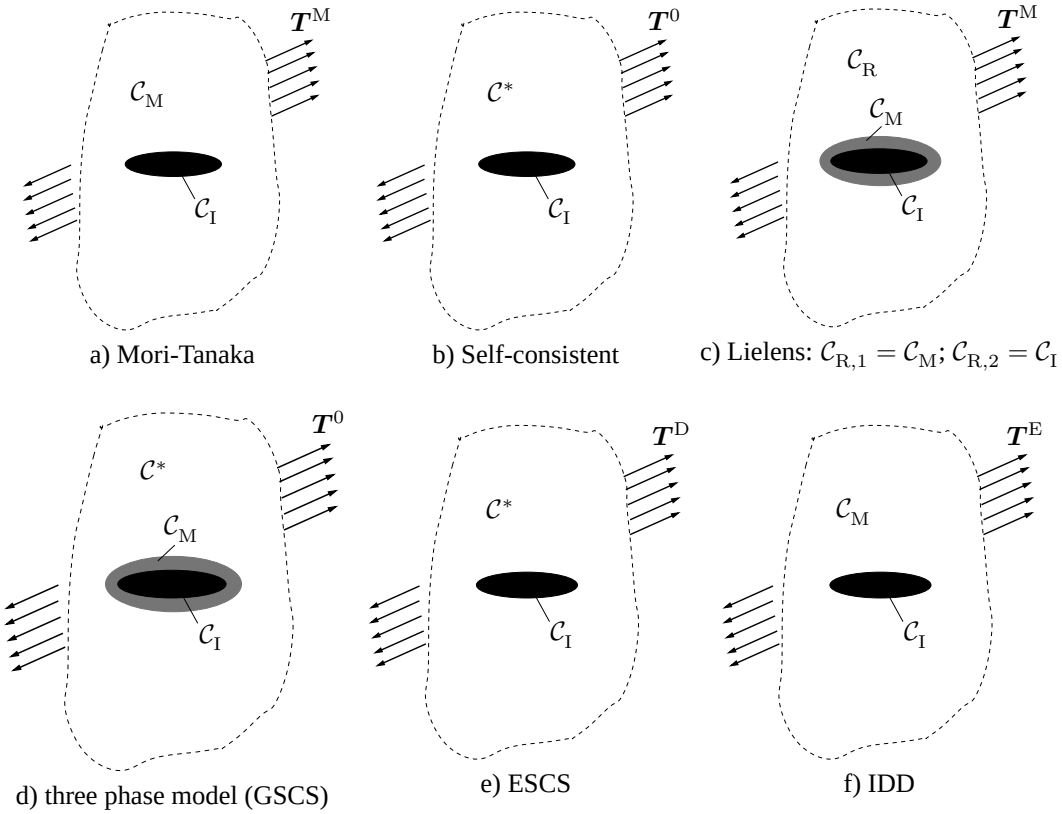

a) Mori-Tanaka b) Self-consistent c) Lielens: $\mathcal{C}_{\mathrm{R},1} = \mathcal{C}_{\mathrm{M}}; \mathcal{C}_{\mathrm{R},2} = \mathcal{C}_{\mathrm{I}}$

d) three phase model (GSCS) e) ESCS f) IDD

Figure 1: A schematic overview on different homogenization schemes for estimating the average stress or strain, respectively.

2.2 Hashin-Shtrikman bounds

Following the approach of Hashin and Shtrikman (1963) leads to the equation for the upper and lower bound of the elasticity tensor for a two-phase material:

$$\mathcal{C}^{*}_{(\mathrm{HS}+)} = \mathcal{C}_{\mathrm{I}} + c_{\mathrm{M}} \left[(\mathcal{C}_{\mathrm{M}} - \mathcal{C}_{\mathrm{I}})^{-1} + c_{\mathrm{I}} \mathcal{S}_{\mathrm{I}} \mathcal{C}_{\mathrm{I}}^{-1} \right]^{-1}; \quad \mathcal{C}^{*}_{(\mathrm{HS}-)} = \mathcal{C}_{\mathrm{M}} + c_{\mathrm{I}} \left[(\mathcal{C}_{\mathrm{I}} - \mathcal{C}_{\mathrm{M}})^{-1} + c_{\mathrm{M}} \mathcal{S}_{\mathrm{M}} \mathcal{C}_{\mathrm{M}}^{-1} \right]^{-1}. \quad (14)$$

As can be seen the upper Hashin-Shtrikman bound corresponds to the Mori-Tanaka result. The upper bound can also be obtained with the Mori-Tanaka method just by interchanging matrix and inclusion material.

2.2.1 Lielens method

Lielens (1999) proposed the following interpolative homogenization model for a two-phase material:

$$\mathcal{C}^{*}_{(\mathrm{LIL})} = \left[\left(1 - \frac{c_{\mathrm{I}} + c_{\mathrm{I}}^{2}}{2} \right) \mathcal{C}^{*-1}_{(\mathrm{MT}^{-1})} + \frac{c_{\mathrm{I}} + c_{\mathrm{I}}^{2}}{2} \mathcal{C}^{*-1}_{(\mathrm{MT})} \right]^{-1}, \quad (15)$$

in which $\mathcal{C}_{(\mathrm{MT})}$ is the estimation for the effective elasticity from the Mori-Tanaka method. $\mathcal{C}_{(\mathrm{MT}^{-1})}$ is the effective elasticity tensor following from the inverse Mori-Tanaka approximation in which, for a two-phase material, the smaller volume part becomes the matrix material and vice versa. Therefore the Lielens method can be seen as a properly chosen interpolation between the Mori-Tanaka and inverse Mori-Tanaka method and between the Hashin-Shtrikman bounds, respectively. This model is also referred to as the Interpolative Double Inclusion model in literature (e.g. Pierard et al. (2004)).

2.3 Self-consistent scheme

The self-consistent method approximates the interaction between the phases by assuming that each phase is embedded in a infinite volume of an effective medium with elastic properties $\mathcal{C}^{*}$ of the composite. Therefore the

effective elasticity stiffness of the material passes into the matrix stiffness ($\mathcal{C}_{\mathrm{M}} = \mathcal{C}^*$) and we obtain the influence tensor

$$\mathcal{A}_{\mathrm{I(SCS)},i} = \left[\mathcal{I} + \mathcal{S}^* \, \mathcal{C}^{*-1} \left(\mathcal{C}_{\mathrm{I},i} - \mathcal{C}^*\right)\right]^{-1}. \tag{16}$$

Due to the fact that the influence tensor $\mathcal{A}_{\mathrm{I(SCS)},i}$ depends on the effective elasticity tensor $\mathcal{C}^*_{\mathrm{E}}$, the equation is implicit and nonlinear.

$$\mathcal{C}^*_{(\mathrm{SCS})} = \mathcal{C}_{\mathrm{M}} + \sum_i c_i \left(\mathcal{C}_{\mathrm{I},i} - \mathcal{C}_{\mathrm{M}}\right) \mathcal{A}_{\mathrm{I(SCS)},i} \tag{17}$$

Algorithmically, the method requires an additional iterative loop to calculate $\mathcal{C}^*_{(\mathrm{SCS})}$. In general, the self-consistent method gives a sufficient prediction of the behavior of polycrystals but it is less accurate in the case of two-phase composites as shown by (Pierard et al., 2004, see).

3 ESCS and IDD approach

3.1 Effective self-consistent scheme (ESCS)

The effective self-consistent scheme (ESCS), proposed by Zheng and Du (2001) is based on the three-phase model. In the three-phase model the average stress $\langle \boldsymbol{T} \rangle_i$ over all type-i inclusions is estimated by that a single inclusion i is embedded in a finite matrix material, the matrix atmosphere, which is in turn embedded in the unbounded unknown effective medium, shown in Figure 2 a). In the following the inclusion together with its matrix atmosphere will be called inclusion-matrix cell and will be denoted by a subscript 'D', which implies that this cell has to be representative for an inclusion distribution.

Shortly recall the assumptions made in order to obtain the effective elasticity tensor for this method. For a more detailed description see Du and Zheng (2002). The volume V is subjected to the uniform stress distribution $\boldsymbol{T}^0$. In the first step it is assumed that the inclusion-matrix cell only consists of the matrix material, leading to stress and strain being uniform according to the Eshelby theorem and taking the form

$$\boldsymbol{E}^{\mathrm{D}}_i = \mathcal{C}^{-1}_{\mathrm{M}} \boldsymbol{T}^{\mathrm{D}}_i, \qquad \boldsymbol{T}^{\mathrm{D}}_i = \left(\mathcal{I} - \Omega_{\mathrm{D}i}\mathcal{H}\right)^{-1} \boldsymbol{T}^0 \tag{18}$$

where $\Omega_{\mathrm{D}i}$ is the eigenstiffness tensor of the cell with respect to the unknown effective medium, and $\mathcal{H}$ describes the compliance increment, defined by

$$\mathcal{H} = \mathcal{C}^{*-1} - \mathcal{C}^{-1}_{\mathrm{M}}. \tag{19}$$

$\Omega_{\mathrm{D}i}$ is calculated by

$$\Omega_{\mathrm{D}i} = \mathcal{C}^*(\mathcal{I} - \mathcal{S}^*_i) \tag{20}$$

where $\mathcal{S}^*_i$ denotes the Eshelby tensor for the cell embedded into the unknown effective material.

In the next step the uniform strain $\boldsymbol{E}^{\mathrm{D}}_i$ has to be incorporated in the original three-phase model problem, by applying extra tractions $\boldsymbol{\tau}^{\mathrm{D}}_i \boldsymbol{n}$, with the outward normal $\boldsymbol{n}$ on the inclusion boundary. This additional stress contribution is calculated by

$$\boldsymbol{\tau}^{\mathrm{D}}_i = (\mathcal{C}_{\mathrm{I},i} - \mathcal{C}_{\mathrm{M}})\boldsymbol{E}^{\mathrm{D}}_i. \tag{21}$$

As depicted in Figure 2 b) and c) the solution of the original problem is thus obtained by the superposition of two seperate problems. A key ingredient in order to establish the ESCS estimate is the approximation of the average stress, denoted by $\boldsymbol{T}^*_i$ within the inclusion for the decomposed problem as shown in Figure 2 c). In Du and Zheng (2002) it has been shown, that this average stress $\boldsymbol{T}^*_i$ can be approximated by an average stress, denoted by $\boldsymbol{T}'_i$, which occurs in a two-phase reference problem where the effective medium is replaced by the matrix material as shown in Figure 2 f). The error due to this approximation is in the second order in c.
By definition, the stress and strain are uniform in the matrix atmosphere in Figure 2 b) and equal to $\boldsymbol{T}^{\mathrm{D}}_i$ and $\boldsymbol{E}^{\mathrm{D}}_i$. Therefore a two-phase model with a single inclusion embedded in the unbounded matrix material is considered, which is subjected to a uniform stress field $\boldsymbol{T}^{\mathrm{D}}_i$ and $\boldsymbol{\tau}^{\mathrm{D}}_i \boldsymbol{n}$ on the boundary of the inclusion. The obtained strain field is constant and equal to $\boldsymbol{E}^{\mathrm{D}}_i$. Therefore the problems in Figure 2 b) and e) are completely equivalent. Next the superposition of the two problems illustrated in Figure 2 e) and f) leads to a much simpler problem of the matrix-inclusion problem. The average stress over the inclusion results in

$$\langle \boldsymbol{T} \rangle^{\mathrm{escs}}_i = \left(\mathcal{I} + \Omega^{\mathrm{M}}_i \mathcal{H}_i\right)^{-1} \left(\mathcal{I} - \Omega_{\mathrm{D}i}\mathcal{H}\right)^{-1} \boldsymbol{T}^0. \tag{22}$$

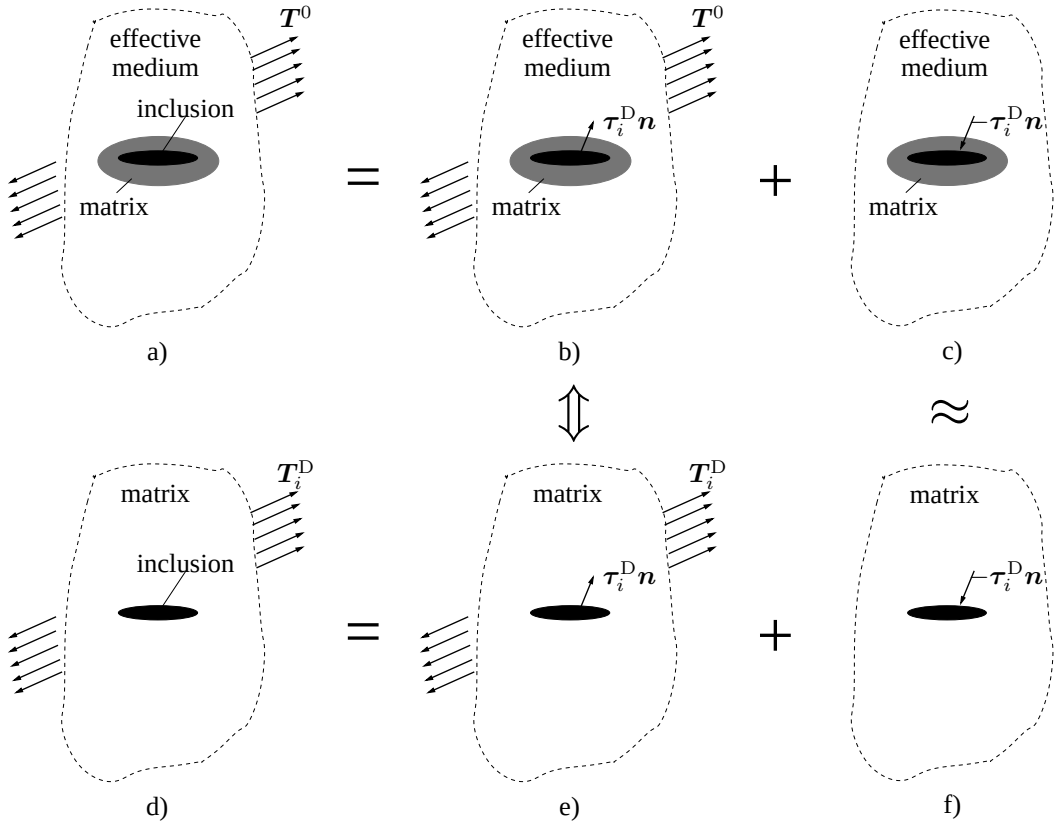

Figure 2: A schematic overview on the ESCS approach (Zheng and Du, 2001).

As mentioned before, the substitution of the problem in Figure 2 c) by e) leads to an error of $O(c^2)$ compared to $\langle \boldsymbol{T} \rangle_i^{\mathrm{escs}}$ and the exact average stress $\langle \boldsymbol{T} \rangle_i$ in the inclusion for the whole estimate. Therefore $\langle \boldsymbol{T} \rangle_i$ can be replaced by $\langle \boldsymbol{T} \rangle_i^{\mathrm{escs}}$. The average strain tensor $\langle \boldsymbol{E} \rangle$ can be expressed by (see Nemat-Nasser and Hori (1993))

$$\langle \boldsymbol{E} \rangle = \mathcal{C}_{\mathrm{M}}^{-1}\, \boldsymbol{E}^0 + \sum_i c_i (\mathcal{C}_i^{-1} - \mathcal{C}_{\mathrm{M}}) \langle \boldsymbol{T} \rangle_i. \tag{23}$$

Adopting the strain-equivalence $\langle \boldsymbol{E} \rangle = \mathcal{C}^{*-1} \boldsymbol{T}^0$ yields to the relation

$$\mathcal{H} \boldsymbol{T}^0 = \sum_i \mathcal{H}_i \langle \boldsymbol{E} \rangle_i, \tag{24}$$

where $\mathcal{H}_i$ are defined as the compliance fluctuations

$$\mathcal{H}_i = \mathcal{C}_i^{-1} - \mathcal{C}_{\mathrm{M}}. \tag{25}$$

Using (25) together with (18) leads to an implicit equation for the compliance increment represented by

$$\mathcal{H} = \mathcal{H}_i^{\mathrm{d}} \left(\mathcal{I} - \Omega_{\mathrm{D}i} \mathcal{H} \right)^{-1} \tag{26}$$

which results in an error of third order dependent of c. $\mathcal{H}_i^{\mathrm{d}}$ can be interpreted as the dilute estimate and is calculated by

$$\mathcal{H}_i^{\mathrm{d}} = \sum_i c_i \left(\mathcal{H}_i^{-1} + \Omega_i^0 \right)^{-1}. \tag{27}$$

This relation can therefore be used to determine the effective elasticity tensor $\mathcal{C}^*$, thereby obtaining the relation

$$\mathcal{C}^*_{(\mathrm{ESCS})} = \left(\mathcal{H} + \mathcal{C}_{\mathrm{M}} \right)^{-1}. \tag{28}$$

Zheng and Du (2001) showed that in the case that all $\Omega_{\mathrm{D},i}$ are identical, denoted by Ω_{D}, the solution of the ESCS method coincides with an effective stress model for the estimation of the average stress over any inclusion, which is embedded in the unbounded matrix material which is subjected to a modified uniform far-field stress $\boldsymbol{T}^{\mathrm{D}}$ given by

$$\boldsymbol{T}^{\mathrm{D}} = \left(\mathcal{I} - \Omega_{\mathrm{D}} \mathcal{H} \right)^{-1} \boldsymbol{T}^0 \tag{29}$$

rather than the real stress $\boldsymbol{T}^0$ which is also the physical explanation for the name prefix *effective* in the term of ESCS.

3.2 Interaction direct derivative (IDD)

Zheng and Du (2001) derived an explicit version for estimating $\mathcal{C}^*$ instead of an implicit equation like (28), namely the interaction direct derivative (IDD) estimate. First the right side of (26) is expanded to

$$\mathcal{H} = \mathcal{H}^{\mathrm{d}} + \sum_i \mathcal{H}_i^{\mathrm{d}} \Omega_{\mathrm{D}i} \mathcal{H}, \tag{30}$$

where $\mathcal{H}^{\mathrm{d}} = \sum_i \mathcal{H}_i^{\mathrm{d}}$. This yields to an error of third order in c. Due to the fact that $\Omega_{\mathrm{D}i}^{\mathrm{M}}$ is an approximation of $\Omega_{\mathrm{D}i}$ with an error of first order in c, this yields to the approximate solution

$$\mathcal{H}^{\mathrm{idd}} = \left(\mathcal{I} - \sum_i \mathcal{H}_i^{\mathrm{d}} \Omega_{\mathrm{D}i}^{\mathrm{M}} \right)^{-1} \mathcal{H}^{\mathrm{d}} \tag{31}$$

and the effective elasticity tensor

$$\mathcal{C}^*_{(\mathrm{idd})} = \left(\mathcal{H}^{\mathrm{idd}} + \mathcal{C}_{\mathrm{M}} \right)^{-1}. \tag{32}$$

This solution is called interactive direct derivative estimate for the effective elasticity tensor $\mathcal{C}^*_{(\mathrm{idd})}$. To estimate the average stress and strain, respectively, of any inclusion, this inclusion is embedded in the matrix material which is subjected to a modified remote boundary traction $\boldsymbol{T}^{\mathrm{E}}\boldsymbol{n}$ with

$$\boldsymbol{T}^{\mathrm{E}} = \left(\mathcal{I} - \sum_i \Omega_{\mathrm{D}i}^{\mathrm{M}} \mathcal{H}_i^{\mathrm{d}} \right)^{-1} \boldsymbol{T}^0 \tag{33}$$

called the effective stress. As can be seen the IDD estimate $\mathcal{C}^*_{(\mathrm{idd})}$ has always an explicit structure, which only involves physical and quantitatively well-defined quantities due to its derivation. The IDD method is valid for any physically possible high concentration of inclusions and is also capable of taking any inclusion distribution into account. If the inclusions are of the same type a much easier form can be obtained (see Zheng and Du (2001)). In this case it can also be shown that the IDD and Mori-Tanaka estimate coincide with each other in the sense of energy-equivalence. Note that

$$\boldsymbol{T}^{\mathrm{M}} = \left(\mathcal{I} - \sum_i \Omega_i^{\mathrm{M}} \mathcal{H}_i^{\mathrm{d}} \right)^{-1} \boldsymbol{T}^0 \tag{34}$$

represents the analogous expression to (33) in the context of the Mori-Tanaka method.

4 Comparison of different homogenization approaches for two-phase composites

Throughout this section we assume that the matrix and inclusion are isotropic and only two-phase composites in isothermal linear elasticity are considered. We compare the prediction of the macroscopic behavior of different classical mean-field homogenization methods with FE results obtained from a RVE. Furthermore we will investigate the prediction of these methods concerning different stiffness ratios of the inclusion-matrix pair. Finally a comparison is made regarding the ESCS and IDD method.

Firstly the well-known mean field homogenization methods for two different stiffness ratios over the inclusion concentration are investigated. Figure 3 shows the predicted macroscopic elastic modulus E^* for a combination of $E_{\mathrm{M}} = 210$ GPa and $E_{\mathrm{I}} = 430$ GPa, where the subscript M is the matrix material and I the inclusion. In the following the Poisson ratio is assumed to be $\nu = 0.25$ for all phases. The concentration c describes the volume fraction of the inclusion. Figure 4 shows the predicted macroscopic elastic modulus E^* for a combination of $E_{\mathrm{M}} = 21$ GPa and $E_{\mathrm{I}} = 210$ GPa.

As expected the different methods deviate distinctly from each other for a higher contrast in the material properties of the matrix and inclusion. For a small contrast, as shown in Figure 3 for a ratio of $\sim$2, only small differences in the prediction of the elastic modulus using the different methods can be seen. In this context we would like to emphasize the well-known fact, that the Voigt-bound represents the maximum upper bound whereas the Reuss-bound defines the minimum lower bound of the stiffness. Voigt and Reuss method predict in general a distinct different Young's modulus, which can already been seen for a small stiffness ratio. Numerous narrow bounds are provided by the Hashin-Shtrikman bounds where all other predictions are located. To be able to distinguish better between the different homogenization methods, we investigate the different methods on Figure 4 where the

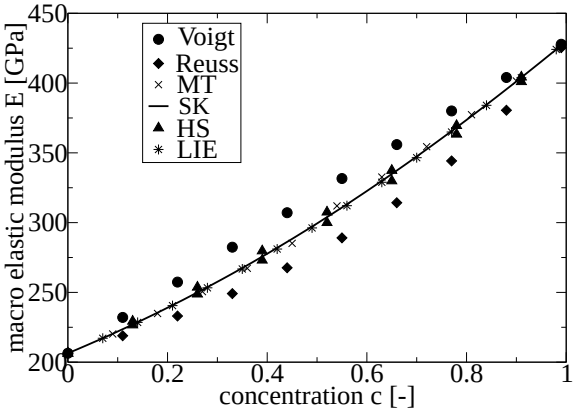

Figure 3: Prediction of effective Young's modulus E^* with different homogenization methods for $E_{\mathrm{M}} = 210$ GPa, $E_{\mathrm{I}} = 430$ GPa and $\nu = 0.25$. (MT = Mori-Tanaka; SCS = self-consistent; HS = Hashin-Shtrikman bounds; LIE = Lielens methods)

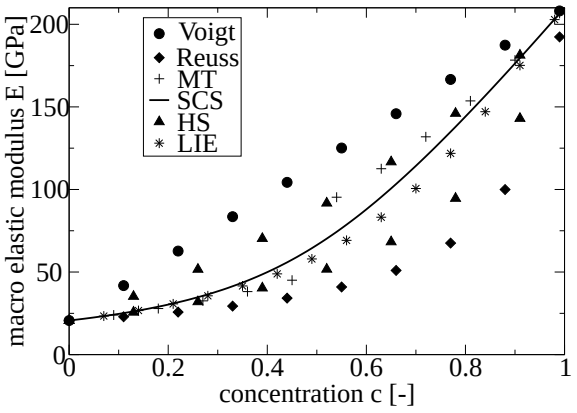

Figure 4: Prediction of effective Young's modulus E^* with different homogenization methods for $E_{\mathrm{M}} = 21$ GPa, $E_{\mathrm{I}} = 210$ GPa and $\nu = 0.25$. (MT = Mori-Tanaka; SCS = self-consistent; HS = Hashin-Shtrikman bounds; LIE = Lielens methods)

predictions are done for a stiffness ratio of 10. Here the difference between the methods is more clearly visible over the volume fraction. In this case the Hashin-Shtrikman bounds are also quite far from each other. The Mori-Tanaka method shows a jump in the predicted elastic modulus for concentrations around 50 % which results from the fact that in the Mori-Tanaka scheme the matrix material is defined as the material having the higher concentration. This shows that, depending on which material is considered to be the matrix material, the Mori-Tanaka estimate coincides with the lower (for matrix = softer material) or the upper (for matrix = harder material) Hashin-Shtrikman bound.

For a small volume fraction of inclusions up to 30% the Mori-Tanaka, self-consistent and Lielens estimate nearly coincide with each other. However,reason with increasing volume fraction the difference in the predictions is rather pronounced. The reason for this is the different approximation of the effective properties which leads to errors from the first order upwards in c. This leads to wrong predictions for high volume fractions. Physically it is not possible to realize higher volume fractions than 74%, as known for face-centered cubic crystal structure, for equal spherical inclusions without letting the inclusion spheres intersect each other. It has been proven that the Mori-Tanaka method is generally incorrect for higher concentrations of inclusions in Castañeda and Willis (1995). But it is hard to decide whether the Lielens estimate or the self-consistent scheme provide better results for higher volume fractions. A comparison with the obtained FE-results of ideal spherical inclusion for volume fractions up to 30% will be provided later in this section.

Further analyses of these homogenization methods for different stiffness ratios and concentrations are presented in the following. Figure 5 to 10 provide 3D-surface plots of the prediction for the different methods for stiffness ratios up to 20. Due to the fact that it is not possible to compare the behavior over different stiffness ratios by plotting the surfaces above each other, in Figure 11 and 12 the resulting effective elastic modulus E^* normalized by E_{M} over the stiffness ratio of inclusion and matrix material is shown.

As can be seen from the surface plots, the behavior of the homogenization methods over different stiffness ratios is changed for different concentrations of the inclusion volume fraction c, however, the general behavior remains the same. The Voigt estimate shows a linear dependence of the effective elastic modulus with respect to the volume fraction of the inclusion representing an upper bound as mentioned before. The Reuss estimate is the lower bound which only shows an increase of the effective elastic modulus in the end. Afore it remains at a nearly constant level. The same behavior can be observed for the upper and lower Hashin-Shrikman bounds only at a higher or lower level, respectively. For a relatively low volume fraction of inclusion the Lielens and self-consistent estimate coincide result in curves showing only small increase of E^*/E_{M} with respect to $E_{\mathrm{I}}/E_{\mathrm{M}}$. For a huge amount of inclusions ($c = 0.8$) both methods deviate from each other, where the self-consistent shows a nearly linear behavior with increasing stiffness ratio, whereas the Lielens estimate shows a more quadratic behavior. Both are quite close to the Hashin-Shtrikman bounds which is depicted for high concentration c of inclusions in Figure 4. As can be seen by interpretation of Figure 12, the stiffness ratio has an immense effect on the effective properties, especially at high volume fractions of inclusion, and therefore the homogenization methods should also be checked for their behavior for high stiffness ratios as done here, instead of solely investigating their behavior at different volume

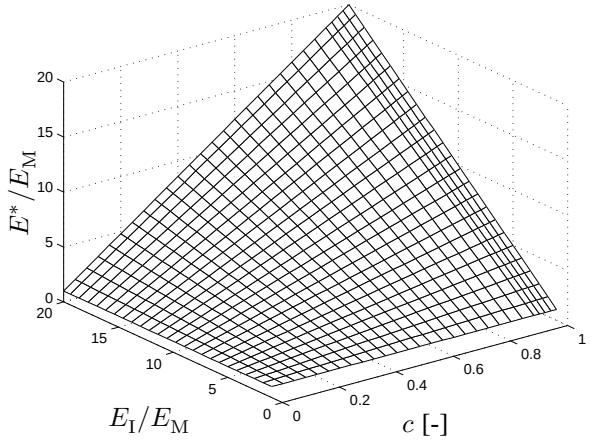

Figure 5: Prediction of effective Young's modulus E^* of Voigt method for different concentrations c and stiffness ratios $E_\mathrm{I}/E_\mathrm{M}$

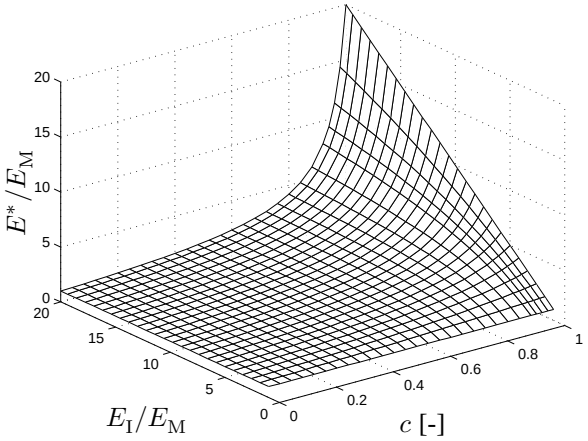

Figure 6: Prediction of effective Young's modulus E^* of Reuss method for different concentrations c and stiffness ratios $E_\mathrm{I}/E_\mathrm{M}$

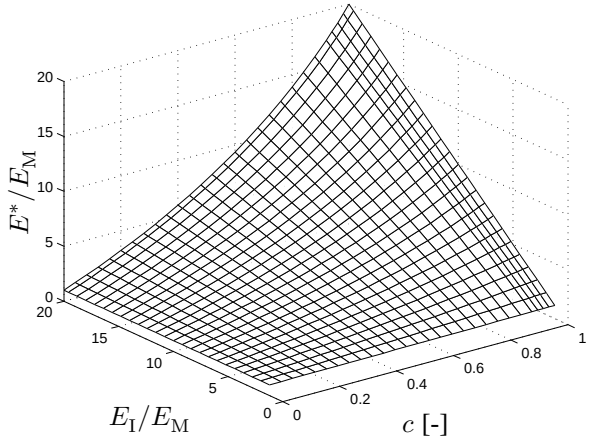

Figure 7: Prediction of effective Young's modulus E^* of Hashin-Shtrikman upper bound for different concentrations c and stiffness ratios $E_\mathrm{I}/E_\mathrm{M}$

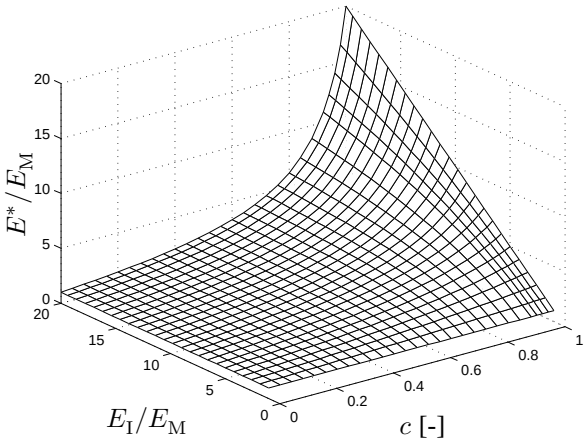

Figure 8: Prediction of effective Young's modulus E^* of Hashin-Shtrikman lower bound and Mori-Tanaka estimate, respectively, for different concentrations c and stiffness ratios $E_\mathrm{I}/E_\mathrm{M}$

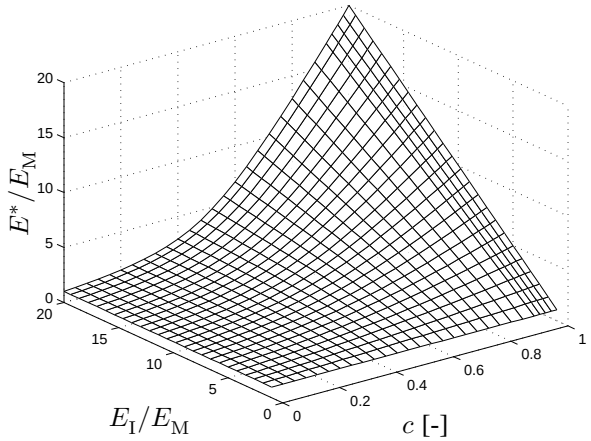

Figure 9: Prediction of effective Young's modulus E^* of self-consistent method for different concentrations c and stiffness ratios $E_\mathrm{I}/E_\mathrm{M}$

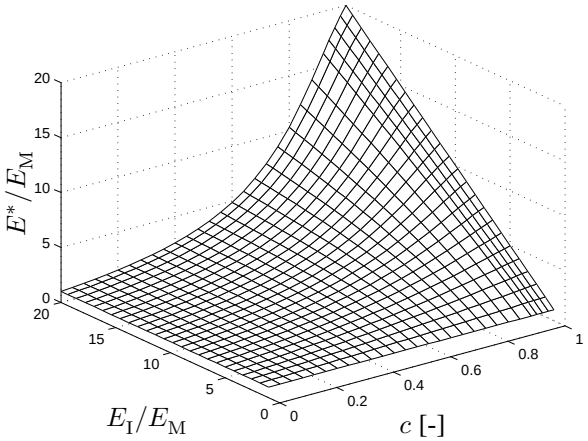

Figure 10: Prediction of effective Young's modulus E^* of Lielens method for different concentrations c and stiffness ratios $E_\mathrm{I}/E_\mathrm{M}$

fractions.

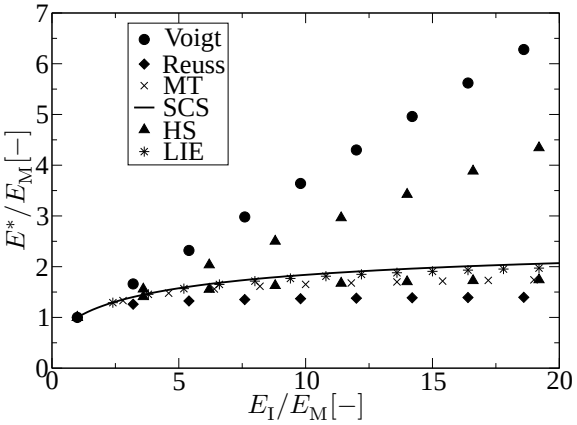

Figure 11: Prediction of effective Young's modulus E^* with different homogenization methods for different stiffness ratios $E_{\mathrm{I}}/E_{\mathrm{M}}$ for $c = 0.3$

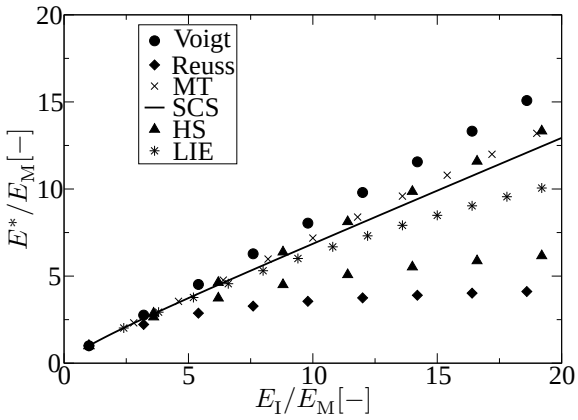

Figure 12: Prediction of effective Young's modulus E^* with different homogenization methods for different stiffness ratios $E_{\mathrm{I}}/E_{\mathrm{M}}$ for $c = 0.8$

4.1 Comparison with FE-results

Before we compare these well-known homogenization methods with the ESCS and IDD estimate, first the so far obtained results are compared with Finite-Element simulations. For this purpose RVEs with randomly distributed inclusions are generated for different volume fractions using the software DIGIMAT. The model is generated by successively placing randomly distributed equally sized spheres into the matrix material until the desired volume fraction with the desired number of spheres or voids is reached. If a randomly placed sphere intersects another already placed sphere, it is attempted to place that particular sphere differently using yet another random generator. The resulting models with spherical inclusion are shown in Figure 13 and with spherical voids in Figure 14. The FE simulations were done with the software ABAQUS/Standard applying linear displacement boundary conditions to three faces of the model such that these are fixed in their respective normal direction so that every degree of freedom is fixed on one single face. The displacement is applied on another face in its normal direction.

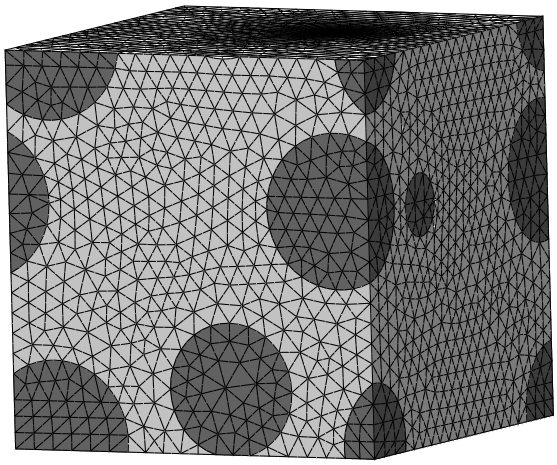

Figure 13: RVE with randomly distributed spherical inclusion of a volume fraction $c = 0.2$

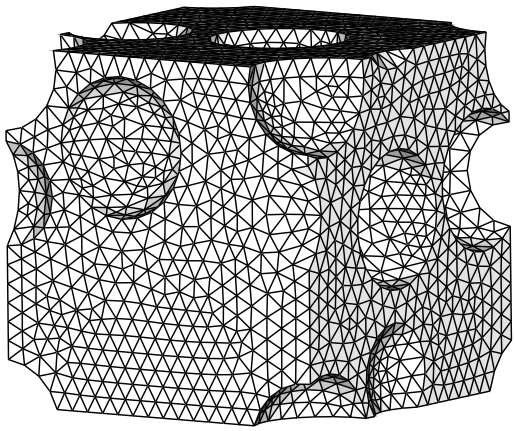

Figure 14: RVE with randomly distributed voids of a volume fraction $c = 0.2$

In Figure 15 the results of the different homogenization methods are compared for a stiffness ratio $E_{\mathrm{I}}/E_{\mathrm{M}} = 10$ with the obtained results from the FE-simulation up to a inclusion volume fraction of $c = 0.35$. It can be stated that for the case of spherical isotropic inclusion the Lielens method shows the best agreement for higher inclusion volume fractions which was also earlier found by Pierard et al. (2004). But as seen from Figure 16 with increasing stiffness ratio $E_{\mathrm{I}}/E_{\mathrm{M}}$, the FEM-results yields to a softer behavior as the Lielens method but it still predicts the best agreement compared to the other methods.

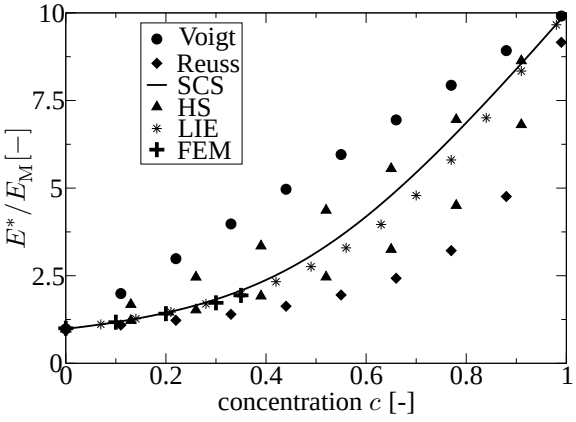

Figure 15: Comparison of homogenization results for effective Young's modulus E^* with FEM-results for $E_\mathrm{M} = 21$ GPa, $E_\mathrm{I} = 210$ GPa and $\nu = 0.25$.

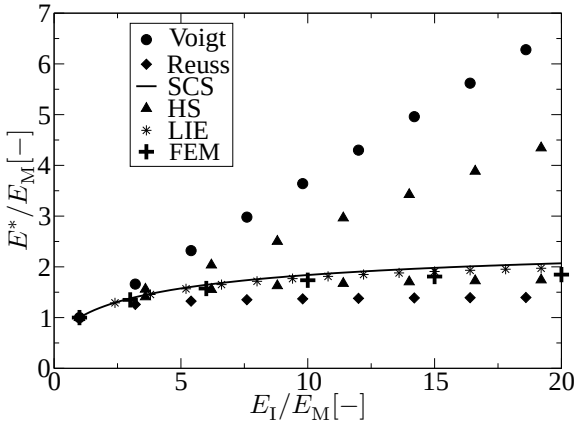

Figure 16: Comparison of homogenization results for effective Young's modulus E^* with FEM-results for different stiffness ratios $E_\mathrm{I}/E_\mathrm{M}$ for $c = 0.3$

4.2 Investigation of ESCS and IDD approach

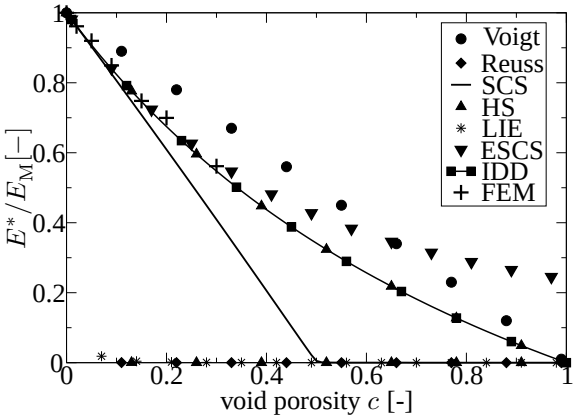

Figure 17: Comparison of different homogenization results and numerical evaluation for the effective Young's modulus E^* of homogenously distributed spherical voids embedded in an isotropic matrix.

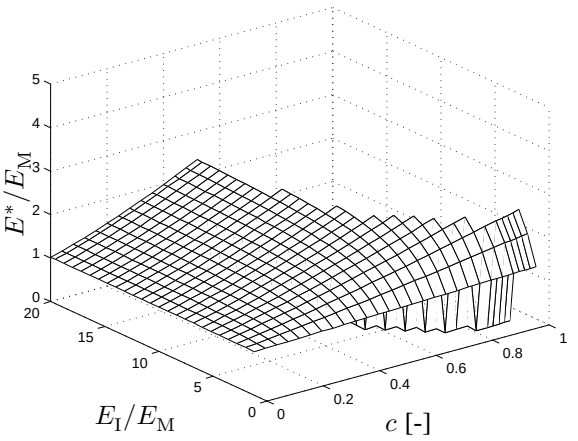

Figure 18: Prediction of effective Young's modulus E^* of ESCS method for different concentrations c and stiffness ratios $E_\mathrm{I}/E_\mathrm{M}$

Now investigating the ESCS and IDD method, in order to verify the implementation of both approaches. Therefore the effective Young's modulus E^* is calculated for an isotropic matrix containing spherical holes, to compare these results with results obtained by Zheng and Du (2001). Figure 17 shows the resulting effective Young's modulus E^* over the void porosity c for $\nu = 0$. For comparison, we also plot the corresponding self-consistent scheme, Lielens method, Hashin-Shtrikman, Voigt and Reuss bounds as well as the numerical results obtained from FEM-simulations. The Reuss bound as well as the Hashin-Shtrikman lower bound and Lielens method provide inappropriate results, so that they are not useful for vanishing stiffness of one phase. The self-consistent scheme also predicts a very soft behavior, where the maximum permitted porosity is $c = 0.5$. The ESCS method does not predict a complete loss of stiffness at $c = 1$ which is of course inappropriate. Here it is clear that this method is only valid for small void porosity c.
It can be seen that the IDD method agrees perfectly with the Mori-Tanaka method or Hashin-Shtrikman upper bound, respectively. Zheng and Du (2001) showed that the IDD method provides for the most materials the best agreement with numerical simulations, especially for $c \to 1$. The here presented results agree quite well with their reported results.

Therefore in the following the behavior of the ESCS and IDD method is investigated regarding isotropic homo-

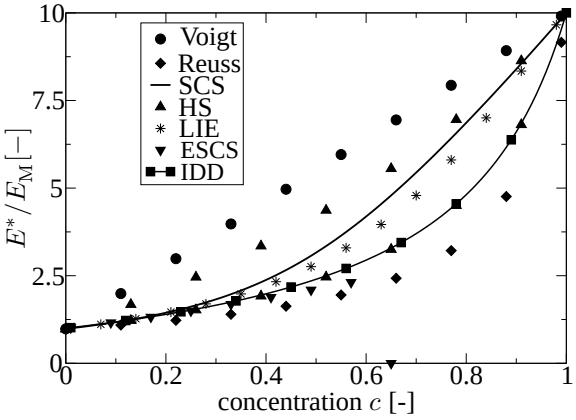

Figure 19: Comparison of homogenization results for effective Young's modulus E^* for $E_{\mathrm{M}} = 21$ GPa, $E_{\mathrm{I}} = 210$ GPa and $\nu = 0.25$.

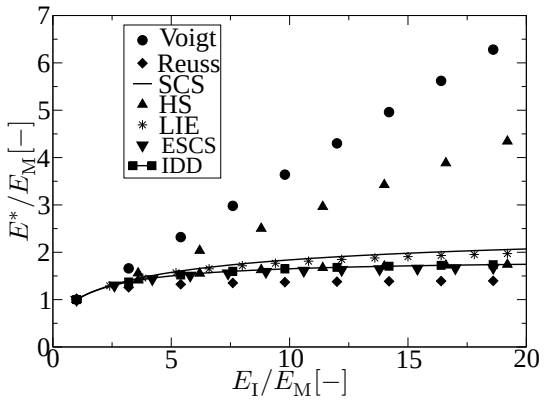

Figure 20: Comparison of homogenization results for effective Young's modulus E^* for different stiffness ratios $E_{\mathrm{I}}/E_{\mathrm{M}}$ for $c = 0.3$

geneously distributed spherical inclusion embedded in an isotropic matrix for different stiffness ratios. In Figure 19 the predicted effective Young's modulus E^* is shown over the inclusion volume fraction c for a stiffness ratio $E_{\mathrm{I}}/E_{\mathrm{M}} = 10$. As can be seen for the case of voids, the IDD method agrees with the Mori-Tanaka estimate. The ESCS predicts a lower effective stiffness ratio E^* than the IDD method. Although both methods predict for $c = 0.3$ and a stiffness ratio $E_{\mathrm{I}}/E_{\mathrm{M}} = 10$ the same effective Young's modulus, with increasing stiffness ratio the ESCS methods predicts a slightly lower result as shown in Figure 20. Furthermore the ESCS method has its numerical limits in predicting the effective behavior. Investigating the behavior in Figure 18 shows that this limit depends on both factors, inclusion volume fraction and stiffness ratio. Therefore this method provides only good results for low stiffness ratios and low volume fractions, moreover this method is more complex than the IDD method. The results found here from numerical analysis confirm the results analytically done by Du and Zheng (2002) where the effective elasticity tensor, here exemplary for the Young's modulus E, fulfills the following conditions:

$$\begin{aligned} E_{\mathrm{SCS}} \leq E^* \leq E_{\mathrm{idd}} \leq E_{\mathrm{ESCS}} \quad &\text{as} \quad E_{\mathrm{I}} \leq E_{\mathrm{M}} \\ E_{\mathrm{ESCS}} \leq E_{\mathrm{idd}} \leq E^* \leq E_{\mathrm{SCS}} \quad &\text{as} \quad E_{\mathrm{M}} \leq E_{\mathrm{I}} \end{aligned} \tag{35}$$

Here it should also be mentioned that the Ponte Castañeda-Willis (PW) estimate (cf. Castañeda and Willis (1995)) coincides with the IDD-method if all inclusion-matrix cells have identical shape and orientation for identical inclusion-interaction distribution, however, the PW does not have an explicit form in all cases which makes the IDD estimate more favorable.

5 Summary and Outlook

In this paper, a number of standard homogenization methods are reviewed and their behavior is compared. The comparison was performed with regard to the inclusion volume fraction, which can usually be found in the literature, but also regarding the contrast in the elastic constituents. It was shown that the contrast has a significant influence on the estimates of these methods and therefore has to be taken into consideration. Results obtained from FEM were compared with these predictions and it was shown that especially the Lielens method agrees quite well with the FEM results.

Furthermore two relatively new approaches, the ESCS and IDD method, were recalled and compared to the classical homogenization results. The results obtained show that a further analysis of the IDD method especially in comparison to the Mori-Tanaka estimate, is reasonable due to its formulation. The IDD estimate has an explicit structure, with a physical explanation of the involved components and it is valid for multiphase composites. It also takes into account the influence of the interaction between inclusions and their surrounding matrix. Formally the method has a universally applicable form to various inclusion distributions. Therefore this method fulfills the main requirements on homogenization methods as mentioned before. A comparison with the RAHS by Guinovart-Díaz et al. (2005) concerning transverse isotropy, a first stage of modeling anisotropy of the effective medium by including concentric circular cylindrical fibers, is an interesting point of investigation to verify the applicability of the presented methods. Further comparisons concerning different inclusion properties as well as inclusion shapes and including anisotropy represent work in progress and will be reported on in future work.

Acknowledgement

Partial financial support for this work provided by the German Science Foundation (DFG) under contract SFB 708 (see http://www.sfb708.uni-dortmund.de) is gratefully acknowledged.

References

Benveniste, Y.: A new approach to the application of Mori-Tanaka's theory in composite materials. *Mechanics of Materials*, 6, 2, (1987), 147–157.

Castañeda, P. P.; Willis, J. R.: The effect of spatial distribution on the effective behavior of composite materials and cracked media. *Journal of the Mechanics and Physics of Solids*, 43, 12, (1995), 1919–1951.

Christensen, R. M.: A critical evaluation for a class of micro-mechanics models. *Journal of the Mechanics and Physics of Solids*, 38, 3, (1990), 379–404.

Du, D.; Zheng, Q.: A further exploration of the interaction direct derivative (IDD) estimate for the effective properties of multiphase composites taking into account inclusion distribution. *Acta Mechanica*, 157, (2002), 61–80.

Eshelby, J. D.: The determination of the elastic field of an ellipsoidal inclusion, and related problems. *Proceedings of the Royal Society of London*, 241, 1226, (1957), 376–396.

Gross, D.; Seelig, T.: *Bruchmechanik, mit einer Einführung in die Mikromechanik*. Springer, Berlin, Heidelberg, 4th edn. (2001).

Guinovart-Díaz, R.; Rodríguez-Ramos, R.; Bravo-Castillero, J.; Sabina, F. J.; Otero-Hernández, J. A.; Maugin, G. A.: A recursive asymptotic homogenization scheme for multi-phase fibrous elastic composites. *Mechanics of Materials*, 37, 11, (2005), 1119–1131.

Hashin, Z.; Shtrikman, S.: A variational approach to the theory of the elastic behaviour of multiphase materials. *Journal of the Mechanics and Physics of Solids*, 11, 2, (1963), 127–140.

Lielens, G.: Micro-Macro modeling of structured materials, Universite Catholique de Louvain (1999), PhD thesis.

Mercier, S.; Molinari, A.: Homogenization of elastic-viscoplastic heterogeneous materials: Self-consistent and Mori-Tanaka schemes. *International Journal of Plasticity*, 25, 6, (2009), 1024–1048.

Mura, T.: *Micromechanics of Defects in Solids*. Martinus Nijhoff, The Hague, The Netherlands, 2nd edn. (1982).

Nemat-Nasser, S.; Hori, M.: Bounds and estimates of overall moduli of composites with periodic microstructure. *Mechanics of materials*, 15, 3, (1993), 163–181.

Nemat-Nasser, S.; Hori, M.: *Micromechanics: overall properties of heterogeneous materials*. Elsevier, Amsterdam, 2nd edn. (1999).

Pierard, O.; Friebel, C.; Doghri, I.: Mean-field homogenization of multi-phase thermo-elastic composites: a general framework and its validation. *Composites Science and Technology*, 64, 10-11, (2004), 1587–1603.

Zheng, Q. S.; Du, D. X.: An explicit and universally applicable estimate for the effective properties of multiphase composites which accounts for inclusion distribution. *Journal of the Mechanics and Physics of Solids*, 49, 11, (2001), 2765–2788.

Address: Dipl.-Ing. Benjamin Klusemann and Prof. Dr. rer. nat. Bob Svendsen, Institute of Mechanics, TU Dortmund, D-44227 Dortmund.
email: benjamin.klusemann@tu-dortmund.de; bob.svendsen@tu-dortmund.de.